**SANDIA REPORT**
SAND2011-8489
Unlimited Release
November 2011

# Mechanisms for Charge-Transfer Processes at Electrode/Solid-Electrolyte Interfaces

Farid El Gabaly, Anthony H. McDaniel, Josh A. Whaley, William Chueh, Roger L. Farrow and Kevin F. McCarty

Prepared by
Sandia National Laboratories
Albuquerque, New Mexico 87185 and Livermore, California 94550

Sandia National Laboratories is a multi-program laboratory managed and operated by Sandia Corporation, a wholly owned subsidiary of Lockheed Martin Corporation, for the U.S. Department of Energy's National Nuclear Security Administration under contract DE-AC04-94AL85000.



Issued by Sandia National Laboratories, operated for the United States Department of Energy by Sandia Corporation.



Available to DOE and DOE contractors from
U.S. Department of Energy
Office of Scientific and Technical Information
P.O. Box 62
Oak Ridge, TN 37831

Telephone: (865) 576-8401
Facsimile: (865) 576-5728
E-Mail: reports@adonis.osti.gov
Online ordering: http://www.osti.gov/bridge

Available to the public from
U.S. Department of Commerce
National Technical Information Service
5285 Port Royal Rd.
Springfield, VA 22161

Telephone: (800) 553-6847
Facsimile: (703) 605-6900
E-Mail: orders@ntis.fedworld.gov
Online order: http://www.ntis.gov/help/ordermethods.asp?loc=7-4-0#online

SAND2011-8489
Unlimited Release
November 2011

# Mechanisms for Charge-Transfer Processes at Electrode/Solid-Electrolyte Interfaces

Farid El Gabaly, Anthony H. McDaniel, Josh A. Whaley, William Chueh, Roger L. Farrow[1] and Kevin F. McCarty

Sandia National Laboratories
P.O. Box 969
Livermore, CA 94550

**Abstract**

This report summarizes the accomplishments of a Laboratory-Directed Research and Development (LDRD) project focused on developing and applying new x-ray spectroscopies to understand and improve electric charge transfer in electrochemical devices. Our approach studies the device materials as they function at elevated temperature and in the presence of sufficient gas to generate meaningful currents through the device. We developed hardware and methods to allow x-ray photoelectron spectroscopy to be applied under these conditions. We then showed that the approach can measure the local electric potentials of the materials, identify the chemical nature of the electrochemical intermediate reaction species and determine the chemical state of the active materials. When performed simultaneous to traditional impedance-based analysis, the approach provides an unprecedented characterization of an operating electrochemical system.

[1] Current address: JDS Uniphase Corporation, Milpitas, CA.

## ACKNOWLEDGMENTS

The authors thank Mark Linne for his efforts in starting this project and Sarah Allendorf for nurturing its accomplishments.

# CONTENTS



# FIGURES

# 1. INTRODUCTION

This report summaries the accomplishments of a Laboratory-Directed Research and Development (LDRD) project focused on developing and applying new in-situ x-ray spectroscopies to understand and improve electric charge transfer in electrochemical devices such as fuel cells. Electrochemical technology will play an increasingly critical role in meeting the nation's energy challenges in both stationary and transportation applications [1-3]. The essential physical phenomenon occurring in all electrochemical devices is the transfer of electrical charge across material interfaces. How this charge transfer occurs and its relationship to the device's performance and reliability is largely unknown. This project developed fundamental understanding of interfacial charge transfer by characterizing it in real time during electrochemical operation. We studied the charge-transfer process in solid-oxide fuel cells (SOFCs) for three reasons: (1) SOFC interfaces are more accessible for in-situ characterization than in other electrochemical devices. (2) Within the same technology platform, electricity can be generated from chemical fuels and vice versa when run as fuel cells [4] or as electrolyzers [5]. (3) SOFCs can operate on a variety of fuels, including hydrogen and hydrocarbons. Thus, SOFCs could potentially contribute significantly toward low-carbon energy systems for both fixed and portable (transportation) applications [4]. But like all electrochemical-based technologies, they suffer from performance and cost issues. The advances needed, especially those for lower-temperature vehicular operation, have been hampered by inadequate understanding of elementary processes. In particular, detailed, microscopic measurements of interfacial species concentrations, their spatial distributions, and transport rates under operating conditions have not been made.

In the project we developed a new approach, electrochemical x-ray photoelectron spectroscopy (EC-XPS) to characterize SOFC materials during operation. The approach required developing new hardware capable of applying electric bias and heating the SOFC devices in the equipment available at the Advanced Light Source (ALS) at Lawrence Berkeley National Laboratory (LBNL). Our approach studied the device materials as they functioned at elevated temperature and in the presence of sufficient gas to generate meaningful currents through the device. We then showed that the EC-XPS approach can measure the local electric potentials of the materials, identify the chemical nature of the electrochemical intermediate species and determine the chemical state of the active materials. When performed simultaneous to traditional impedance-based analysis [6], the approach provides an unprecedented characterization of an operating electrochemical system. In this report we summarize these accomplishments.

# 2. ACCOMPLISHMENTS

## 2.1. Development of a fixture for electrochemical XPS

We developed a versatile fixture that heats and makes reliable electrical contacts to electrochemical devices (see Fig. 1). It is compatible with the type of manipulators commonly used in ultrahigh vacuum chambers. In addition, the fixture enables the spectroscopic characterization of devices in operando, as they, for example, undergo electrochemical reactions with gas-phase species at near-ambient pressure.

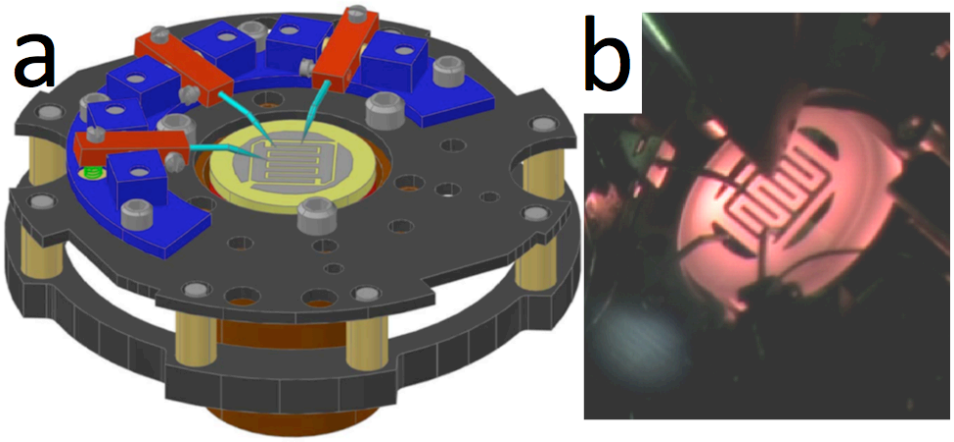


**Figure 1. Fixture for applying three independent electrical contacts to electrochemical devices in traditional vacuum systems. a). Probes (aqua) are contacted against the patterned electrodes (grey) on the electrochemical device using springs (green). The device rests on a resistive heater. b). Photograph showing the fixture operating a hot solid-oxide electrolyte device with Pt working, reference and counter electrodes. The cone collects photoelectrons into the differentially pumped energy analyzer of ALS beamline 11.0.2.**

Our design was constrained to be compatible with the endstations on beamlines 9.3.2 and 11.0.2 at the Advanced Light Source (ALS) that are used for ambient-pressure x-ray photoelectron spectroscopy (APXPS) [7,8]. The sample manipulators on both endstations use STLC™ series hardware manufactured by Thermionics Vacuum Products Company. Samples are mounted on a "platen" that has transferrable electrical contacts. Figure 1(a) presents our modification of a standard Thermionics platen. Three assemblies around the platen's perimeter use spring-loaded probes to make electrical contact to a planar electrochemical device and also hold it against a heater. By accommodating the device's thermal expansion, the spring loading maintains low-impedance electrical contacts and provides good thermal contact to the heater while avoiding cracking brittle materials such as solid-oxide electrolytes [4]. The small contact area of the probes minimizes heat conduction from the device. The stiff tungsten probes maintain their shape for tens of hours at high temperature, while a Au-Pd alloy coating protects against corrosion in reactive atmospheres and improves electrical conductance. A 0.5"-diameter ceramic heater compatible with both oxidizing and reducing environments is located at the center of the fixture. Figure 1(b) shows the platen mounted with a planar device fashioned from metal electrodes patterned on a yttria-stabilized-zirconia (YSZ) disk, operating at ~700°C in a $H_2O/H_2$ ambient at ~0.5 torr. Figure 2 shows the electrical configuration. A description of the fixture has been published [9]. In addition to the application examples given in sections 2.2, 2.3 and 2.4, the fixture has been used to examine the electrochemical redox of ceria ($CeO_{2-x}$) [10,11].

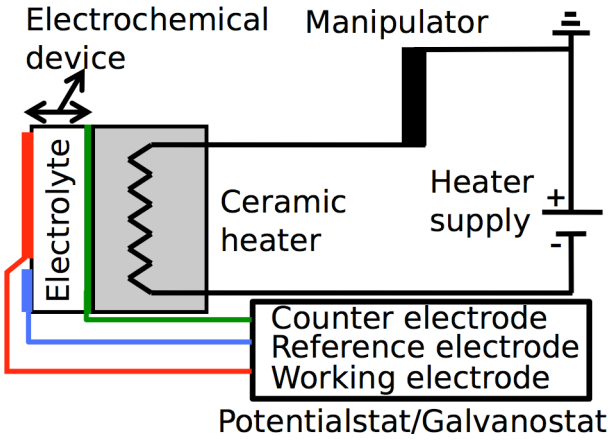


**Figure 2. Electrical circuit used for electrochemical operation and characterization. The illustrated device on the 0.5"-diameter heater has the working and counter electrodes on the top and bottom, respectively, of the electrolyte disk.**

## 2.2. Development of a non-contact method for measuring local electric potential

The fundamental electrochemical phenomenon in both fuel cells and electrolyzers is the formation of electrical double-layers across material interfaces, as illustrated in Fig. 3. Driven by gradients in their chemical and electrical potentials, charged species (electrons and ions) cross through the double-layers from one phase to another. Every double-layer has an associated potential (difference) that is modified by an "overpotential" when the current is flowing. In fact, the current through a double-layer depends exponentially on its overpotential. An overpotential always decreases the device's power output by reducing the useful potential obtained from a fuel cell and increasing the potential needed to drive an electrolyzer. If the overpotential grows relatively fast with increasing current, the device is inefficient and must be run at low current to minimize the losses. We developed a method of using XPS to measure the local electric potential of a material. Measuring the potential jump across abutted materials directly gives the overpotentials. A description of this approach has been published [10,12].

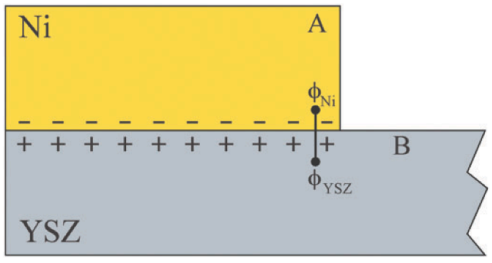


**Figure 3. Schematic of an electrical double-layer at the interface between a metal (Ni) and a solid-state electrolyte (YSZ). The inner potentials on either side of the interface are labeled. XPS data from representative points A and B are used to determine the overpotential of the interface.**

We developed the method using the model device of dense, patterned electrodes on a dense electrolyte as a simplification of the porous and composite materials frequently used in

commercial devices (see Fig. 4) [13]. The electrolyte of the solid-oxide electrochemical cell (SOEC) studied was a wafer of single-crystal YSZ. The Pt (99.99% pure) and Ni (99.995% pure) electrodes were fabricated on the YSZ by evaporation from crucibles heated by an electron beam under high vacuum conditions. The electrode shape was controlled using a stainless-steel shadow mask positioned in front of the YSZ substrate.

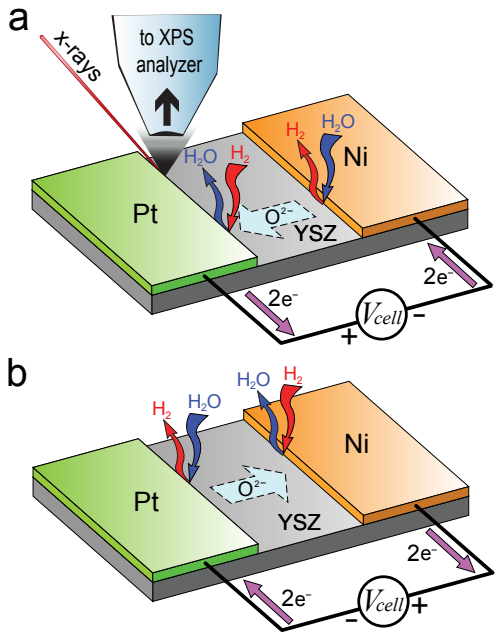


**Figure 4. Schematic of the driven solid-oxide electrochemical cell used in this work. (a) and (b) show the two possible polarities and the gas-phase reactions at each three-phase boundary. (a) also shows the x-ray beam and the collection cone of the spectrometer.**

The fixture described above was used to electrically contact the SOEC while at high temperature in the $H_2O/H_2$ ambient. The holder uses spring-loaded probes to provide reliable electrical contact to the thin-film electrodes and is equipped with a ceramic button-heater compatible with oxidizing atmospheres. A computer-based Gamry potentiostat (model PCI4-750) was used to bias the SOEC and perform standard electrochemical tests.

For obtaining the local electrical potentials of the cell, APXPS spectra were obtained at several values of applied bias. The potentials from the YSZ electrolyte and the Ni and Pt electrodes were measured using the Ni 3p3/2, Zr 3d5/2 and Pt 4f7/2 XPS core levels, respectively. These element-specific core levels have sharp XPS peaks and have relatively high cross-sections for the exciting x-rays (490 eV). The peaks were background corrected and fitted to determine their kinetic energies. At each discrete analysis location, the peak positions with and without applied bias were subtracted. The 910 µm-wide region of YSZ electrolyte (see Fig. 4) between the electrodes was analyzed using 182 Zr 3d5/2 spectra separated by 5 µm steps.

In Fig. 6a the discontinuities in the potentials at the electrode/electrolyte boundaries are the overpotentials. Because the electrodes are metals, their electrical potential is constant. Thus, the metal has the same potential at the point probed by XPS and at its buried interface with the YSZ. We use the 1D spatial resolution of the imaging electron detector to measure the inner potential of the bare YSZ (Fig. 5), which is about 10 µm from the electrode. The YSZ potential at this

point and the potential of the YSZ under the electrode differ only by the small ohmic drop through the short YSZ segment. Figure 6b plots the measured overpotentials for several $V_{cell}$ values.

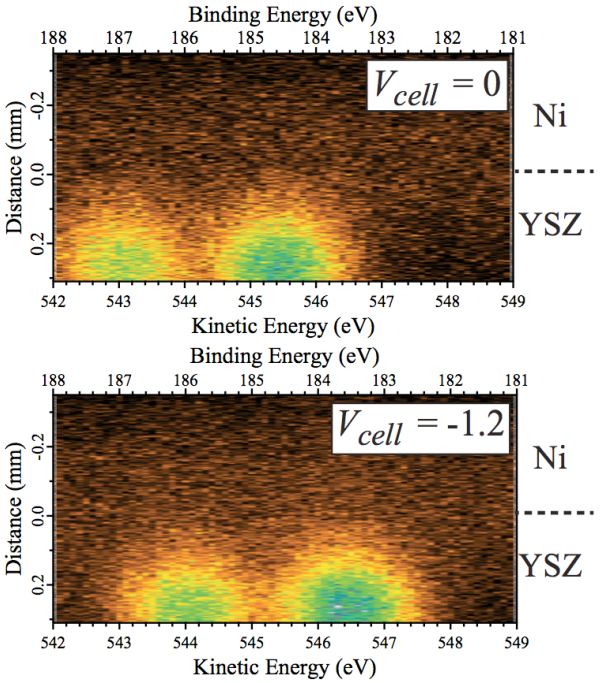


**Figure 5. Example of a rigid shift in the kinetic energy of a XPS peak when bias is applied across the Ni and Pt electrodes. In the image, the Zr 3d doublet ends at the boundary between the YSZ electrolyte and the grounded Ni electrode. The Zr 3d doublet shifts some fraction of the cell bias $V_{cell}$ because the YSZ inner potential changes when a double-layer forms under the Ni electrode.**

To summarize this section, we demonstrated that photo-electron spectroscopy performed in operando at near-ambient pressure can measure directly the individual overpotentials in solid-state electrochemical devices. In our simple electrically driven SOEC, the Ni and Pt electrodes are at the same temperature, see the same gas, and have the same symmetric geometry on the YSZ electrolyte. We can then interpret the origins of the changes in the individual over-potentials with applied bias in terms of the different electro-catalytic activities of Ni and Pt for the $H_2O$ splitting and $H_2$ oxidation reactions. We find without ambiguity that $H_2O$ splitting is faster than $H_2$ oxidation on Ni, while the $H_2$ oxidation reaction on the Pt proceeds more rapidly than $H_2O$ splitting. In addition, by measuring the portion of the applied bias that is consumed at the Ni/YSZ interface, we can determine if the Ni at that interface is oxidized under different conditions. This subject is discussed next.

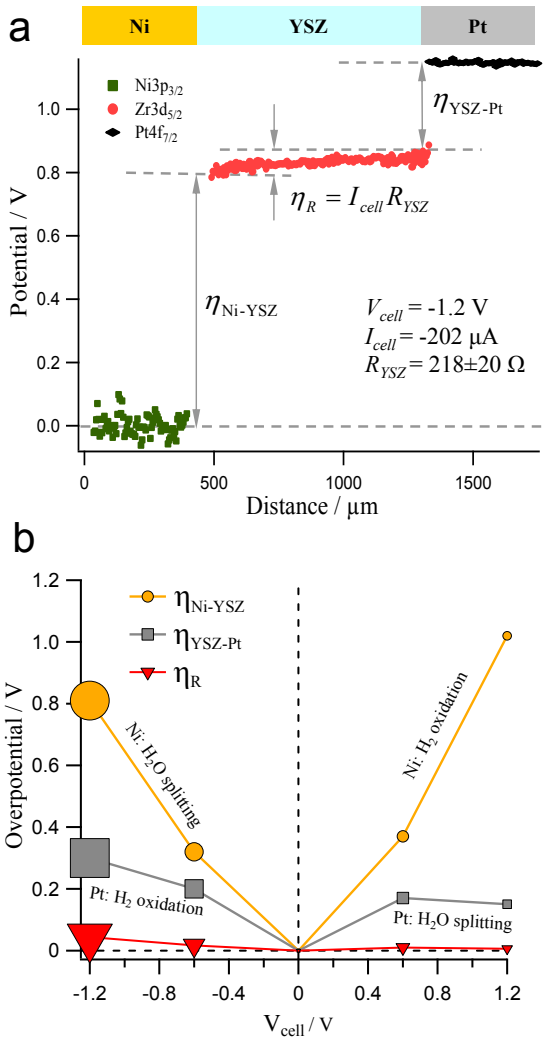


**Figure 6. (a) Potential landscape of the SOEC at $V_{cell}$ = -1.2 V. The labeled overpotentials for the Ni/YSZ and YSZ/Pt interfaces appear as discontinuities in the potential. (b) Measured, absolute values of the three total overpotentials vs. cell bias. The plot labels give the net reactions taking place at each electrode for the given condition. The marker size is proportional to the cell current, $I_{cell}$.**

## 2.3. Observing electrochemical intermediate reaction species

The charge-transfer reactions on solid-oxide electrochemical cells (SOEC) have been the focus of multiple studies over the past decades, both experimental and theoretical. Mechanistic insight has come largely from fitting macroscopic observables such as currents vs. reactant pressure or voltages to non-unique models of rate-equations. While this ”macroscopic” approach has generated considerable insight, it has not unambiguously resolved the chemical nature of the reactions that transfer charge [14]. The main open questions are what are the intermediate reaction steps, which adsorbed species occur in the slow (rate-limiting) steps and where the different reactions occur, i.e., on the metal electrode or the solid-oxide electrolyte. Answering these questions of what and where provides the basic knowledge needed to develop faster and more efficient processes.

A traditional method for elucidating reaction mechanisms is to identify the chemical reaction intermediates using spectroscopy. In principle spectroscopic approaches can identify adsorbed electrochemical reaction intermediates. However, applying surface-sensitive spectroscopies to SOEC systems has large challenges, including high operational temperatures (550 to 1000 °C), the significant gas pressures needed to generate sufficient gas-surface reactions to give meaningful ion currents through the electrolytes, and the fact that the charge-transfer reactions are believed to occur at or very close (normally within 10 to 200 nm) to the interface between the metallic electrode, the ceramic electrolyte and the gas phase. In addition to chemical spectroscopy, complete characterization of the reaction mechanisms requires simultaneous measurements of the electric potential across the materials as a function of cell current, as described in section 2.2.

We have shown that the new electrochemical implementation of x-ray photoelectron spectroscopy (EC-XPS) performed at near ambient pressure can determine the chemical nature of the key reaction intermediate in a gas/solid electrochemical system in operando. We studied the prototypical solid-state system of a YSZ electrolyte with Pt contacts performing the important reactions of $H_2$ oxidation reaction and $H_2O$ electrolysis. Figures 7a and b show photographs of the SOEC device. Figure 7c shows a typical spatially resolved EC-XPS measurement of the oxygen 1s (O1s) core-level photoelectron peak as directly obtained from the two-dimensional detector of the electron energy analyzer. The photoelectrons are dispersed horizontally by binding energy and vertically by distance between the two Pt electrodes. Figure 8 re-plots the spectral information as conventional spectra from 13 evenly spaced positions between the Pt working electrode at position (0) and counter electrode at positions (11) and (12). The spectra reveal that four different oxygen-containing species are present, labeled as: (a) water vapor, (b) surface hydroxyl (OH), (c) lattice ("bulk") oxygen in YSZ, and (d) Pt oxide.

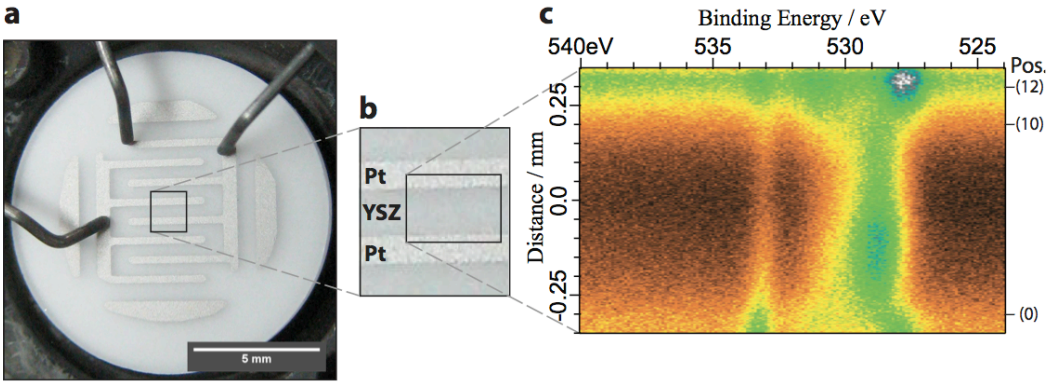


**Figure 7 a) Photograph of the Pt/YSZ/Pt SOEC used in this work. The probes coming from the left and upper right are the electric contacts to the thin-film Pt interdigitated electrodes. b) Zoom in of the region analyzed by XPS. c) Spatially resolved EC-XPS measurement of the oxygen 1s core-level from the boxed region in panel b). The photoelectron intensity is mapped onto a false color scale. Data acquired with the cell hot in the $H_2O/H_2$ mixture but without applied** bias.

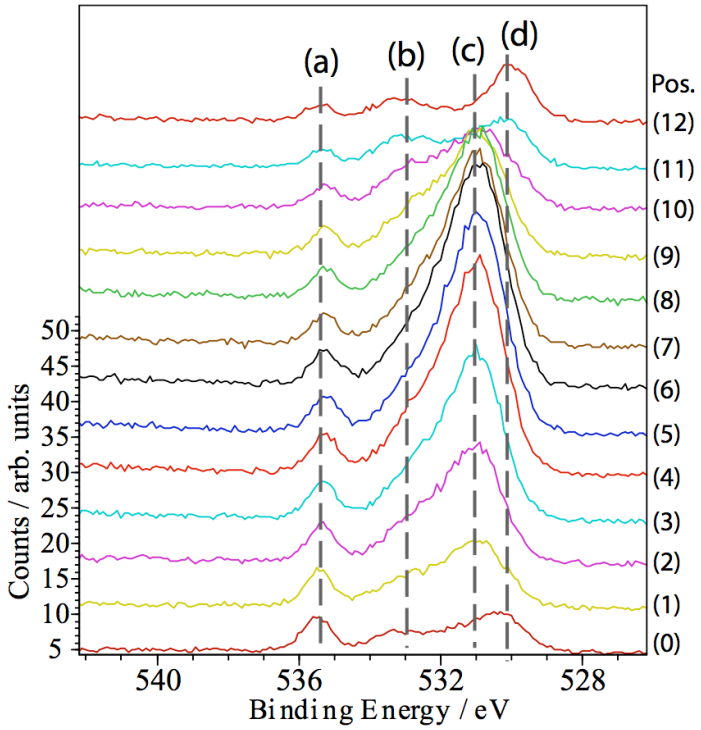


**Figure 8. Spatially resolved EC-XPS spectra obtained by binning the electrons into 50-μm-wide segments between the Pt electrodes. Positions are numbered from the Pt WE (0) to the Pt CE (12). Spectral components are: (a) water vapor, (b) adsorbed hydroxyl, (c) bulk (lattice) oxygen in YSZ, and (d) Pt oxide.**

Figures 9a and b show O1s spectra from positions (1) and (10), respectively acquired at 550 °C for two different biases applied to the cell with all other conditions unchanged. (For display purposes, the binding energies at different bias are adjusted to keep the Zr 3d5/2 peak at 183 eV.) The adsorbed hydroxyl peak changed at positions (1) and (10) when bias was applied. At the other positions between the Pt electrodes the hydroxyl peak did not change. We can relate the observed chemical changes to the corresponding net reactions at positions (1) and (10). When hydrogen electro-oxidation reaction is occurring, the hydroxyl concentration on YSZ is smaller than at equilibrium (no bias); when $H_2O$ electrolysis is occurring, the hydroxyl concentration on YSZ is higher. These changes provide strong evidence that the YSZ hydroxyl is an intermediate species participating in the electrochemical reactions.

We also used the EC-XPS method to measure how electric potential is distributed across the materials in the operating SOEC. Detailed analysis of the potential drops across the material interfaces, the local ”overpotentials” (see above), reveals that the rate-determining step (rds) is a pure chemical reaction without charge transfer [15]. And the two electrons of the net reactions are transferred separately in steps before and after the rds. This information, combined with the new information about the nature of the intermediate reaction species provides an unprecedented experimental description of the reaction mechanism.

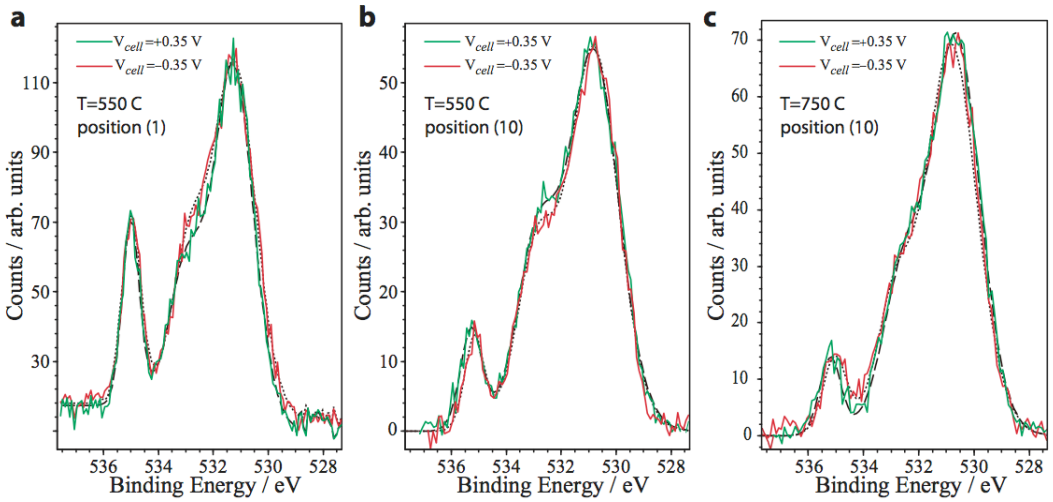


**Figure 9. EC-XPS oxygen 1s spectra at positions (1) and (10), i.e., near the Pt/YSZ/gas interphase, comparing the effect of applied bias on the oxygen-containing species. Green/red lines are the experimental data at $V_{cell}$ = +0.35/ − 0.35 V and dashed/dotted lines are fits to two components, respectively. a) and b). At 550 °C the hydroxyl shoulder changes at positions (1) and (10). c). At 750 °C no change in hydroxyl is observed at position (10).**

## 2.4. Characterizing charge storage in oxidized nickel

Nickel is a common electrode and catalyst in fuel cell and electrolyzer systems [4]. Oxidation of the nickel increases the resistance of the devices, lowering efficiency. So understanding how nickel is oxidized in fuel cell and electrolyzer systems is important. In addition, nickel oxyhydroxides are the charge-storage material in commercial batteries including nickel-metal hydride batteries. In this project we used EC-XPS to analyze the thermal-chemical and electrochemical oxidation and reduction of Ni. We found that oxidation in the presence of $H_2O$ produced NiOOH and an electric potential relative to the Pt counter electrode. Upon discharging the cell (battery), the NiOOH was reduced to Ni metal.

Figure 10 shows a schematic illustration of the cell, where a solid-oxide electrolyte is used to either inject oxygen ions into the Ni or remove the ions. The Pt counter electrode provides oxygen ions and reactions with the gaseous $H_2$ and $H_2O$ provide a source of hydroxyl. Figure 11 shows the result of applying a positive bias of 1.0 V to the Ni electrode. After the external bias is removed, a potential of 80 mV exists across the cell (bottom plot of Fig. 11). That is, the cell is now a battery. The potential remains constant as the cell discharges due to leakage. This establishes that the Ni-containing electrode has two phases in equilibrium. In the example in Fig. 11, the cell was later shorted by the potentiostat. The red and blue lines in the upper plot show the cell current and integrated charge during the discharge, results characteristic of a battery.

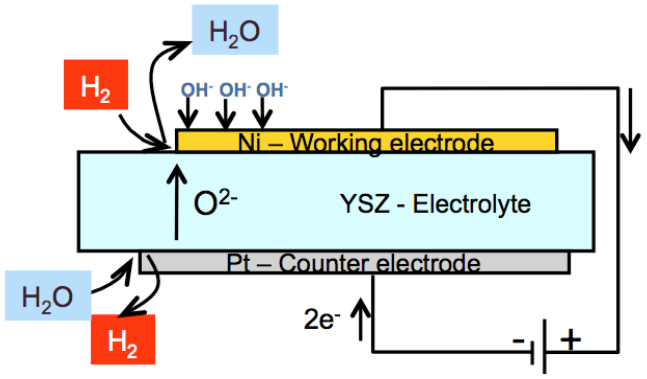


**Figure 10. Schematic illustration of the electrochemical device used to oxidize and reduce Ni in contact with an YSZ electrolyte. The Ni surface is analyzed by XPS during the application of electrical bias.**

The key question, then, is the nature of the oxidized Ni phase that stores charge. We answered this question using EC-XPS. Figure 12 shows the characterization using the Ni 2p core level to provide chemical information. Initially the Ni is metallic (upper spectrum). The middle spectrum shows the partially oxidized Ni while the bottom spectrum shows the fully oxidized (charged) state. Based on literature spectra of standards, we determine that the oxidized Ni is a mixture of Ni metal and NiOOH. We found that we could reversibly take the Ni between the two extremes (metal and NiOOH) by biasing and discharging the cell. Consistently, there are predictions in the literature that the two-phase equilibrium of β-NiOOH and Ni should generate 80 mV potential. This result demonstrates the ability of EC-XPS to determine the charge-storing phases in batteries in operando, which is a powerful approach considering that many of the phases are only stable under the conditions imposed inside the battery, including the electric potential [16].

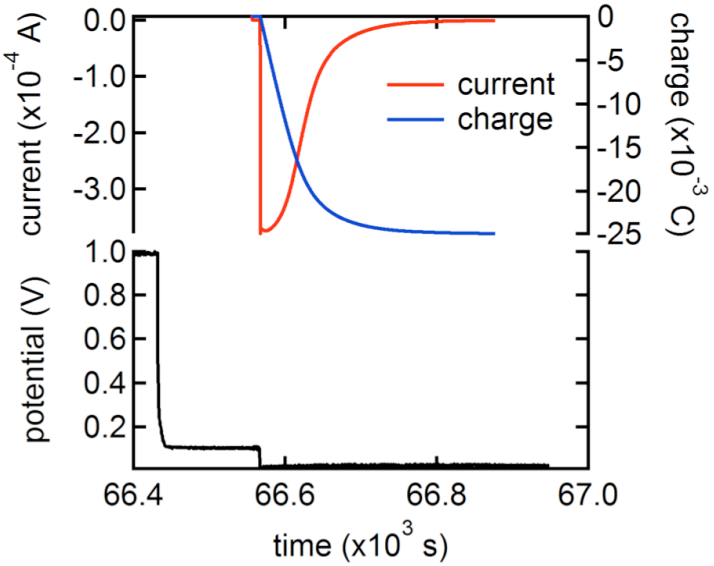


**Figure 11. Electrical characterization showing that electric charge is stored in oxidized Ni. Bottom). Initially the Ni was biased to +1.0 V. After removing the external bias, the cell generated a constant bias of 80 mV, showing that the device was a battery. The cell was then shorted (taking it to 0 V). Top). The current (red) and integrated total charge (blue) during the cell discharge.**

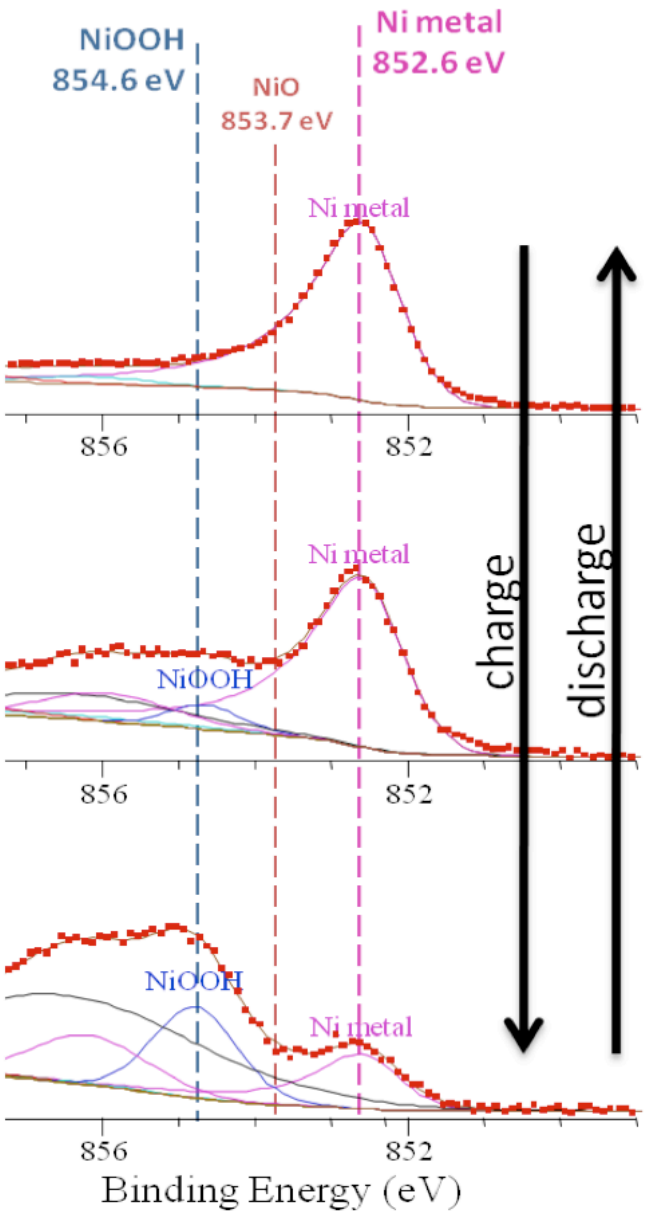


**Figure 12. EC-XPS spectra showing the reversible conversion between Ni metal and NiOOH by biasing and discharging the cell.**

## 2.5. Developing an apparatus with separate environments on two sides of a membrane

The work described above relies on simulating gas-surface reactions and ion current through a solid-state electrolyte by applying a bias to the device immersed in a gas mixture. While useful, this approach has limitations in simulating a real fuel cell or electrolyzer, as discussed next. In these systems, an ion-conducting membrane separates two different gas environments, one containing an oxidizer and the other a fuel. In a single gas environment, fuel cells can't be simulated with $O_2$ as the O source because it reacts with fuels on the exposed Pt heating wire. In

practice the gas mixture in a single environment configuration, such as Figs. 1 and 4, needs to be a fuel and its oxidization product, e.g., $H_2$ and $H_2O$, respectively. In addition, reactions at the two electrodes change the local gas composition. (For example, $H_2O$ electrolysis forms $H_2$ and $O_2$ at one electrode, which may alter the reaction $H_2$ oxidation reaction at the other, adjacent electrode). Because the potential is applied, rather than developed by the separate half cell reactions, the gradients in electrochemical potential can never be the same in the single-environment configuration as in a real fuel cell [17].

In overcome the limitations of the single-gas-environment approach, we developed the ability to perform soft x-ray spectroscopies in a configuration where a membrane separates two different gas environments. Figure 13 provides a schematic of the configuration. A planar electrolyte sealed to a zirconia tube separates the two gas environments, one inside the tube and the other outside. The seal is provided by a special glass developed by Sandia to match the thermal expansion of zirconia. The electrolyte faces the cone of the differentially pumped electron energy analyzer. A backside heater both heats the cell and provides electrical contact to the rear electrode (the counter electrode). Front-side contacts are made by spring-loaded probes (Fig. 13 center), whose positions can be readily moved to contact different electrode geometries. A precision manipulator moves the device in three directions relative to the x-ray beam and the analyzer entrance cone (Fig. 13 right), allowing different regions of the device (electrolyte vs. electrode, for example) to be analyzed. The whole apparatus is modular and transported from Sandia to ALS beamline 11.0.2, where it is installed on a differentially pumped energy analyzer.

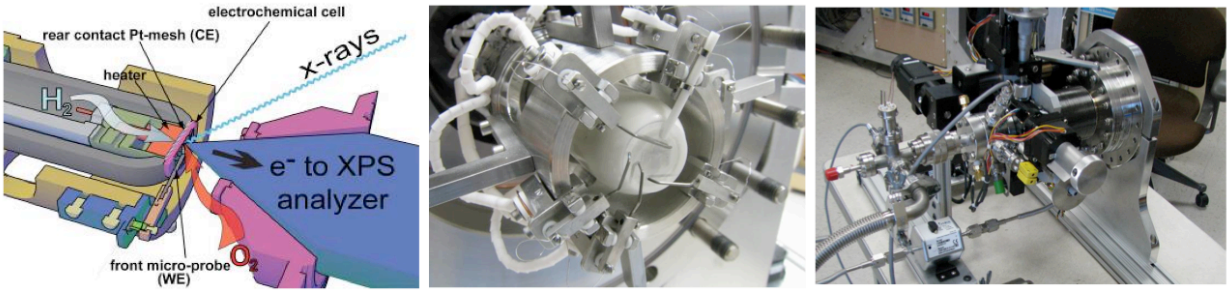


**Figure 13. Custom apparatus for soft x-ray analysis of electrode and electrolyte materials with an ion-conducting membrane separating two separate gas environments. Left). Schematic illustration showing the membrane sealed to a tube inside of which is one gas environment. The front-facing materials are exposed to a separate gas environment and are probed by x-rays during electrochemical operation. Middle). Photograph of the x-ray facing side of the membrane, with spring-loaded probes providing contacts to the electrodes. Right). Photograph showing the external components, including the three-axis manipulator and gas lines.**

A photo-blind diode in a water-cooled housing is used for the fluorescence detection of x-ray absorption spectroscopy (XAS) [18]. The angular position of the diode can be varied by a rotary feed through. In addition to measuring XAS by fluorescence, which probes the bulk of the material, XAS is also measured by photoelectrons collected through the energy analyzer. This electron-yield XAS probes the material's surface. The gas composition on either side of the membrane, the total pressure, the pressure differential across the membrane and the three-axis

positioning are computer controlled. A mass spectrometer provides gas analysis of the x-ray-facing side of the system.

The system was initially tested using the prototypical system of Pt electrodes on a YSZ electrolyte. Figure 14 shows that a true fuel cell is achieved, that is, the device without an electric load generates a potential of about 1 V with $H_2$ and $O_2$ on either sides of the membrane. The cell's power under load is the classis behavior of a fuel cell. This electrical characterization was performed simultaneously to the XPS and XAS analysis of the Pt and YSZ materials.

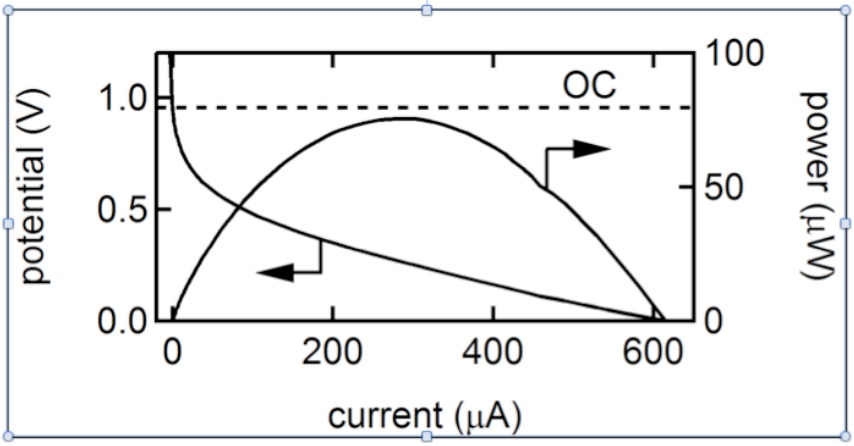


**Figure 14. Demonstration of a fully functioning fuel cell undergoing simultaneous x-ray analysis at the ALS. With no load (zero current), the cell develops about 1 V potential from the separate reactions of $H_2$ and $O_2$ on either side of the membrane. As the cell is loaded, the power increases, reaches a maximum and then decreases, the behavior characteristic of a conventional fuel cell.**

After the initial testing phase, we used the two-environment apparatus to study the state-of-the-art electrocatalysts for the oxygen reduction reaction (ORR) [19] in fuel cells that use solid-oxide electrolytes [20]. Specifically, we studied lanthanum strontium cobalt ferrite [$(La_{1-x}\ Sr_x)\ (Co_{1-y}Fe_y)O_3$, LSCF] and barium strontium cobalt ferrite [$(Ba_{1-x}\ Sr_x)\ (Co_{1-y}Fe_y)O_3$, BSCF]. The single-component change from La to Ba (from LSCF to BSCF) in these perovskite-structure oxides increases the ORR rate substantially (~ 2 orders of magnitude) [21]. The perovskite oxides were deposited on top of the YSZ electrolyte by pulsed laser deposition through shadow masks. Figure 15 shows the geometry and a photograph of the hot cell during x-ray analysis and documents true fuel cell functionality, that is, the development of a Nernst potential.

Both LSCF and BSCF were thoroughly analyzed during fuel-cell operation. XPS was used to examine the composition of the surface while electron-yield and fluorescence-yield XAS were used to determine the oxidation state of metal cations at the surface and in the bulk, respectively. Figure 16 gives the example of the XAS spectra of Co under varying conditions, revealing that the surface Co did not change oxidation state while the bulk Co changed oxidation state with the oxygen pressure. Analysis of the data is in progress and will be presented in a journal publication. We are confident that our work will reveal why BSCF has substantially better reactivity than the same structure with La substitution, i.e., LSCF.

The two-environment apparatus represents the state-of-the-art in photoelectron-based analysis of electrochemical systems. The system provides an unprecedented amount of information, including the composition of the bulk and surface, the oxidation state of the metal cations in the bulk and at the surface, the local electric potentials and the traditional characterization of the device using impedance spectroscopy [6].

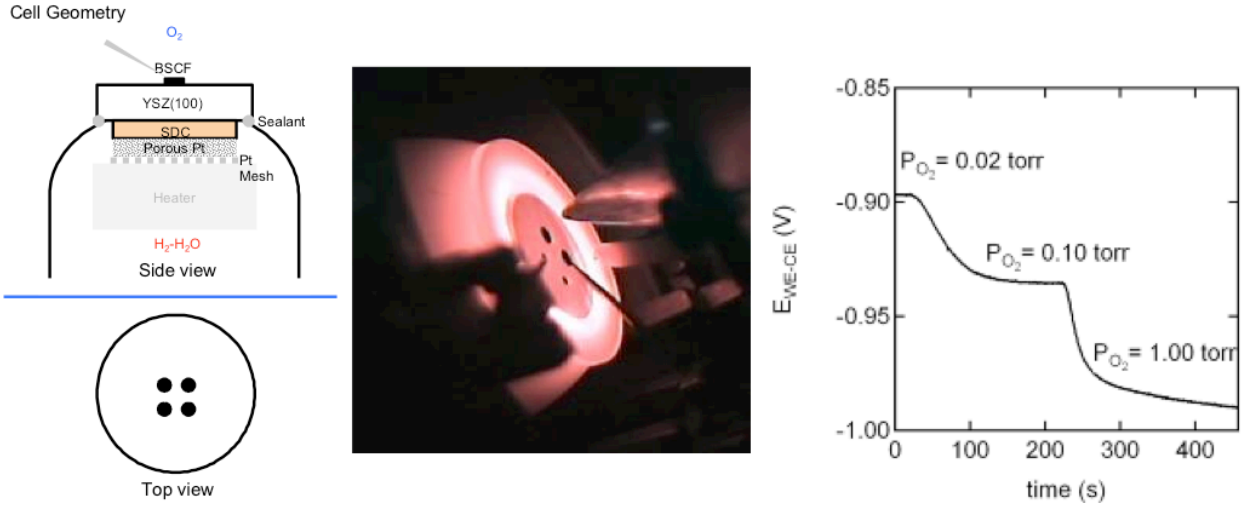


**Figure 15. Left). Schematic illustration of the geometry of the two-environment cell. The disk of YSZ electrolyte was sealed to the YSZ tube using a special glass. Four disk-shaped pads of perovskite were deposited on the top through shadow masks. Center). Photograph of the hot cell immersed in gas at ALS beamline 11.0.2. Probes are contacting two of the electrolyte pads and the cell is positioned in front of the cone of the electron energy analyzer. Right). Potential of the cell as a function of oxygen partial pressure.**

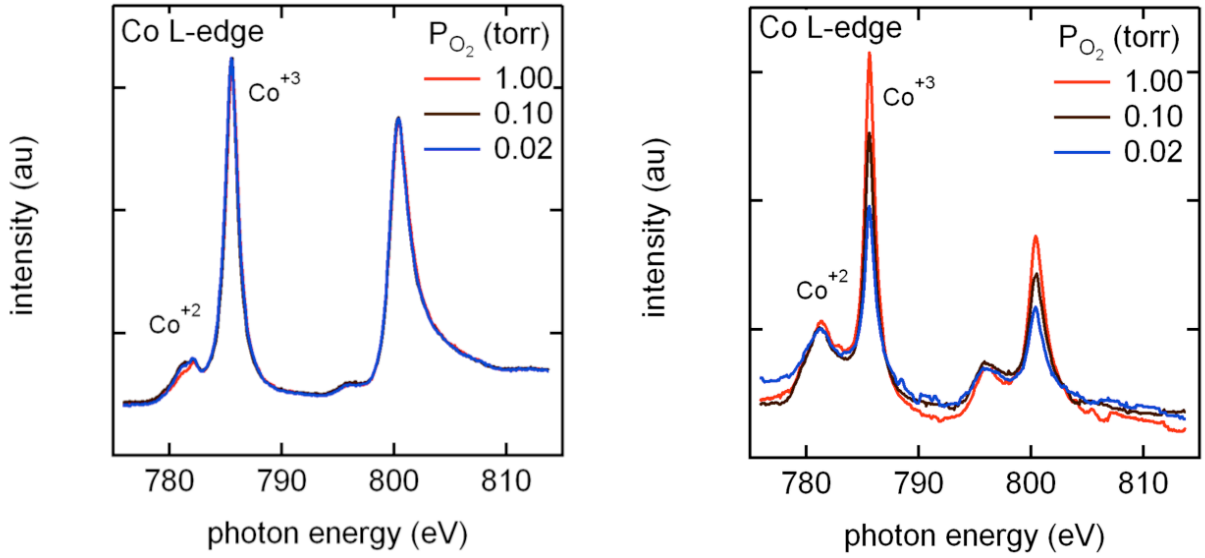


**Figure 16. Example of x-ray absorption spectra (XAS) obtained by scanning the photon energy over the L edge of Co. Left). Surface-sensitive measurement obtained from the yield of secondary electrons. The Co is highly oxidized and does not change state with oxygen pressure in the cell. Center). Bulk-sensitive measurement obtained from emitted photons (fluorescence). The Co becomes markedly more oxidized as the oxygen pressure is increased.**

# 3. CONCLUSIONS

In the LDRD project "Mechanisms for Charge Transfer Processes at Electrode-Solid-Electrolyte Interfaces" we developed a substantially more powerful method to understand electrochemistry that involves gas-phase molecules reacting with solid surfaces. Our approach uses x-rays to provide chemical characterization of the solid materials and their adsorbates. It also determines the local electric potential, information vital to fully measuring the electrochemical potential in devices. The most important attribute of our approach is that the x-ray characterization is performed in operando, that is, as electrons and ions flow through a device with a solid-state electrolyte.

Our specific accomplishments include: 1) the design of a simple yet powerful fixture to heat and apply biases to solid-state electrolytes in a traditional surface-science vacuum chamber, 2) developing a method that uses photoelectrons for the non-contact measurement of local electric potential, 3) the first spectroscopic identification of electrochemical reaction intermediates on a solid-oxide electrolyte, 4) extending the approach to batteries by characterizing the phases that store charge after electrochemical oxidation, 5) designing and building a sophisticated apparatus that performs x-ray characterization of a ion-conducting membrane that separates two gas environments and 6) using the two-environment apparatus to understand the chemical origin of why cation substitution affects electrocatalytic activity of state-of-the-art perovskite-structure materials.

Our approach is ready to be applied to improve the efficiency, reliability and affordability of electrochemical devices such as fuel cells, electrolyzers and the types of batteries that involve solid/gas reactions (such as lithium air batteries [16]).

# 4. REFERENCES


[1] *Basic Research Needs for Electrical Energy Storage: Report of the Basic Energy Sciences Workshop*. (Office of Basic Energy Sciences, U.S. Department of Energy, Office of Basic Energy Sciences, U.S. Department of Energy, 2007).

[2] D. Lindley, "The Energy Storage Problem," *Nature* **463**, 18 (2010).

[3] Electricity from Renewable Resources: Status, Prospects, and Impediments. (National Research Council, Washington, D.C., 2010).

[4] K. Huang and J. B. Goodenough. *Solid oxide fuel cell technology*. (Woodhead Publishing Limited, 2009).

[5] M. Ni, M. K. H. Leung and D. Y. C. Leung, "Technological development of hydrogen production by solid oxide electrolyzer cell (SOEC)," *Int. J. Hydrog. Energy* **33**, 2337 (2008).

[6] M. E. Orazem and B. Tribollet. *Electrochemical Impedance Spectroscopy*. (Wiley, 2008).

[7] D. F. Ogletree, H. Bluhm, E. D. Hebenstreit and M. Salmeron, "Photoelectron spectroscopy under ambient pressure and temperature conditions," *Nucl. Instrum. Methods A* **601**, 151-160 (2009).

[8] M. E. Grass, P. G. Karlsson, F. Aksoy, M. Lundqvist, B. Wannberg, B. S. Mun, Z. Hussain and Z. Liu, "New Ambient Pressure Photoemission Endstation at ALS Beamline 9.3.2," *Rev. Sci. Instrum.* **81**, 053106 (2010).

[9] J. A. Whaley, A. H. McDaniel, F. El Gabaly, R. L. Farrow, M. E. Grass, Z. Hussain, Z. Liu, M. A. Linne, H. Bluhm and K. F. McCarty, "Fixture for characterizing electrochemical devices in-operando in traditional vacuum systems," *Rev. Sci. Instrum.* **81**, 086104 (2010).

[10] C. Zhang, M. E. Grass, A. H. McDaniel, S. C. DeCaluwe, F. El Gabaly, Z. Liu, K. F. McCarty, R. L. Farrow, M. A. Linne, Z. Hussain, G. S. Jackson, H. Bluhm and B. W. Eichhorn, "Measuring fundamental properties in operating solid oxide electrochemical cells by using in situ X-ray photoelectron spectroscopy," *Nat. Mater.* **9**, 944 (2010).

[11] S. C. DeCaluwe, M. E. Grass, C. J. Zhang, F. El Gabaly, H. Bluhm, Z. Liu, G. S. Jackson, A. H. McDaniel, K. F. McCarty, R. L. Farrow, M. A. Linne, Z. Hussain and B. W. Eichhorn, "In Situ Characterization of Ceria Oxidation States in High-Temperature Electrochemical Cells with Ambient Pressure XPS," *J. Phys. Chem. C* **114**, 19853 (2010).

[12] F. El Gabaly, M. E. Grass, A. H. McDaniel, R. L. Farrow, M. A. Linne, Z. Hussain, H. Bluhm, Z. Liu and K. F. McCarty, "Measuring individual overpotentials in an operating solid-oxide electrochemical cell " *Phys. Chem. Chem. Phys.* **12**, 12138 (2010).

[13] A. McDaniel, F. El Gabaly, E. Akhadov, R. L. Farrow, K. F. McCarty, M. A. Linne, S. C. Decaluwe, C. Zhang, B. Eichhorn, G. S. Jackson, Z. Liu, M. Grass, Z. Hussain and H. Bluhm, "In-Situ Investigation of SOFC Patterned Electrodes using Ambient-Pressure X-ray Photoelectron Spectroscopy," *ECS Transactions* **25**, 335-343 (2009).

[14] D. G. Goodwin, H. Y. Zhu, A. M. Colclasure and R. J. Kee, "Modeling Electrochemical Oxidation of Hydrogen on Ni-YSZ Pattern Anodes," *J. Electrochem. Soc.* **156**, B1004 (2009).

[15] E. Gileadi. *Electrode Kinetics for Chemists, Chemical Engineers, and Materials Scientists*. 101 (Wiley-VCH, 1993).

[16] R. A. Huggins. *Advanced Batteries: Materials Science Aspects*. (Springer, 2009).
[17] R. P. O'Hayre, S.-K. Cha, W. G. Colella and F. B. Prinz. *Fuel Cell Fundamentals*. 2nd edn, (Wiley, 2009).
[18] J. Stöhr. *NEXAFS Spectroscopy*. 4 (Springer, 1996).
[19] S. B. Adler, "Factors governing oxygen reduction in solid oxide fuel cell cathodes," *Chem. Rev.* **104**, 4791-4843 (2004).
[20] T. Ishihara (ed.). *Perovskite Oxides for Solid Oxide Fuel Cells*. (Springer Science, 2010).
[21] Z. P. Shao and S. M. Haile, "A high-performance cathode for the next generation of solid-oxide fuel cells," *Nature* **431**, 170 (2004).

# DISTRIBUTION

| | | |
|---|---|---|
| 1 | MS0899 | RIM - Reports Management, 9532 (electronic copy) |
| 1 | MS0123 | D. Chavez, LDRD Office, 1011 (electronic copy) |


Sandia National Laboratories